Computational Prototyping of an RF MEMS Switch using Chatoyant

M. Bails*, J. A. Martinez*, S. P. Levitan*, I. Avdeev**, M. Lovell**, D. M. Chiarulli***

University of Pittsburgh Departments of
*Electrical, **Mechanical Engineering, and ***Computer Science
348 Benedum Hall, Pittsburgh, PA, 15261, USA, mikeb@ee.pitt.edu,
jmarti@ee.pitt.edu, steve@ee.pitt.edu, ivast@pitt.edu, mlovell@pitt.edu, don@cs.pitt.edu

ABSTRACT

In this paper we demonstrate the capabilities of our system-level CAD tool, Chatoyant, to model and simulate an RF MEMS switch. Chatoyant is a mixed signal, multi-domain CAD tool that can be used to design and analyze complete mixed-technology micro-systems. We perform a system level simulation of an RF MEMS switch. This is accomplished by coupling mechanical and electrical domains of this system. We verify our mechanical results using the commercial simulation packages, ANSYS, and CoventorWare.

Keywords: microelectromechanical systems, modeling, microsystems, finite element analysis, radio frequency switch, circuit simulation

1 BACKGROUND

Chatoyant is a multi-domain system level simulation tool. It is optimized for loosely coupled systems incorporating complex components, including electrical, optical, and mechanical devices which are found in multi-domain microsystems [1]. In Chatoyant, the mechanical behaviors of MEMS devices are modeled as a set of differential equations that define their dynamics as a reaction to external forces. Each mechanical element (beam, plate, etc.) is characterized by a template consisting of a combination of mass, damping, and stiffness matrices in a Modified Nodal Analysis (MNA) representation. This template is created by transforming the second order ordinary differential equation (ODE) motion equation into a first order ODE for a piecewise linear (PWL) solution (Figure 1).

General motion equation

$$F = [K][U] + [B][\dot{U}] + [M][\ddot{U}]$$

Standard ODE Transformation

$$\begin{bmatrix} 0 & M \\ M & B \end{bmatrix}\begin{bmatrix} \ddot{U} \\ \dot{U} \end{bmatrix} + \begin{bmatrix} -M & 0 \\ 0 & K \end{bmatrix}\begin{bmatrix} \dot{U} \\ U \end{bmatrix} = \begin{bmatrix} 0 \\ I \end{bmatrix} F$$

Templates for every basic element (e.g. beam)

$$X = \begin{bmatrix} \dot{U} \\ U \end{bmatrix}; \; [Mb]\dot{X} + [Mk]X = [E]F$$

Figure 1: Mechanical Matrix Representation

By controlling the degrees of freedom for the components in the system and using a PWL solver, a trade-off between speed and accuracy is realized. Electrical components are modeled using a similar MNA technique. The interaction between electrical and mechanical components is accomplished by modeling the coupled energy between the domains.

2 RF MEMS DEVICE

The RF MEMS device we model was designed and fabricated at the University of Michigan [2, 3]. It is composed of electrostatic actuation plates and a capacitive plate suspended over a coplanar waveguide by spring meanders (Figure 2). This device works as an electrically switched shunt capacitor. With no voltage applied to the actuation pads, most of the RF signal can pass through the signal line. Applying a voltage to the actuation pads, results in an increase in the coupling capacitance between the signal line and the central capacitive plate. This lowers the impedance between the signal and ground, which effectively "shunts" the RF energy to ground and stops the RF propagation through the signal line [4]. The sensitivity of the device is directly related to the number of meanders in the spring assembly. Increasing the number of meanders will ideally lower the required voltage for switch operation. For this research, we considered a device having four meanders.

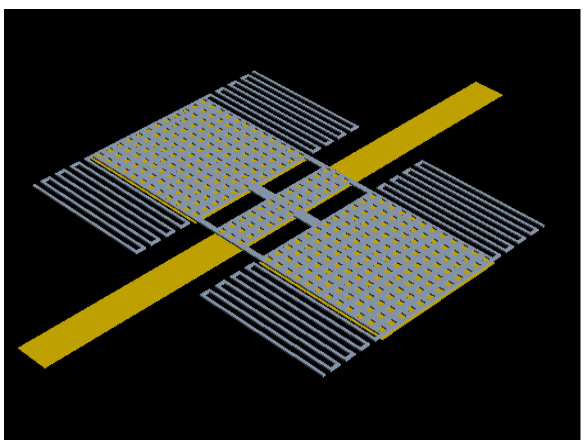

Figure 2: 3-D Rendering of RF MEMS Device

3 MODELING OF RF MEMS DEVICE

The general modeling techniques of Chatoyant are discussed in section 3.1. The remaining subsections are dedicated to the different aspects for prototyping the mechanical features of this device. These investigations include the stiffness properties of the spring meanders, the modal analysis of the spring assembly, and the dynamic analysis of the spring assembly.

The work is part of an ongoing analysis, which will include electrical models and system level analyses. The electrical models will be used to perform pull-in voltage analyses. Finally, a complete system simulation will be performed, including the RF signal, control voltages, and the MEMS switch verifying Chatoyant's mixed-domain capabilities.

3.1 Chatoyant Mechanical Modeling

The mechanical model for the device can be viewed as a set of ordinary differential equations that define its dynamics as a reaction to external forces. Each mechanical element (beam, plate, etc.) is composed of a set of characteristic matrices, K (stiffness), B (damping) and M (mass). Theses matrices are static and independent of the dynamics in the body. Figure 3 shows an example of the stiffness matrix used for a typical 2-D beam element [5]. These matrices can be extended to 3-D structures incorporating six degrees of freedom (x, y, z, rotation x, rotation y, rotation z).

$$K = \frac{EI}{L^3}\begin{bmatrix} 12 & 6L & -12 & 6L \\ 6L & 4L^2 & -6L & 2L^2 \\ -12 & -6L & 12 & -6L \\ 6L & 2L^2 & -6L & 4L^2 \end{bmatrix}$$

Figure 3: Sample 2-D Beam Element Matrix

The standard second order differential equation of motion, where U is position V is velocity and A is acceleration, is given by:

$$F = KU + BV + MA \tag{1}$$

Knowing the velocity is the first derivative and acceleration is the second derivative, the above equation can be reduced to a standard first order form which gives a complete characterization of the mechanical system (see Figure 1).

The use of a PWL general solver decreases the computational task and allows for a trade-off between accuracy and speed. This technique can be used in both electrical and mechanical simulations, which merges the complex device interactions in these mixed domains.

3.2 Four Meander Spring Constant

The spring constant for a four meander spring is determined by applying a known force value (in this case, 1μN) to the free end of the structure and dividing by the resulting displacement. Chatoyant performs a dynamic analysis of the spring stiffness whereas ANSYS [6] and Coventor [7] use static analyses. For this device, the desired movement is in the z-direction, however, it is feasible that unwanted movement in x or y may exist. This unwanted movement could generate coupling variations to the incoming RF signal. Table 1 gives a comparison of the resulting spring constants in the x, y, and z directions for the different solvers, showing good agreement.

	Stiffness (N/m)		
	Kz	Kx	Ky
Chatoyant	0.0543	1.749	0.372
Ansys	0.0527	1.773	0.344
CoventorWare Architect	0.0546	1.863	0.396
CoventorWare Analyzer	0.0568	1.881	0.408

Table 1: Four Meander Spring Stiffness Constant

3.3 Spring Modal Analysis

The modal response of a four meander spring is necessary to determine the maximum frequency of operation for the switch. This is done to ensure that any unwanted resonance that may exist in the system is avoided.

The results of the first nine modal frequencies are shown in Figure 4. Table 2 provides a comparison of runtimes for the modal analysis for the different solvers. These analyses were performed on a P4 3.00 GHz processor with 2GB SDRAM.

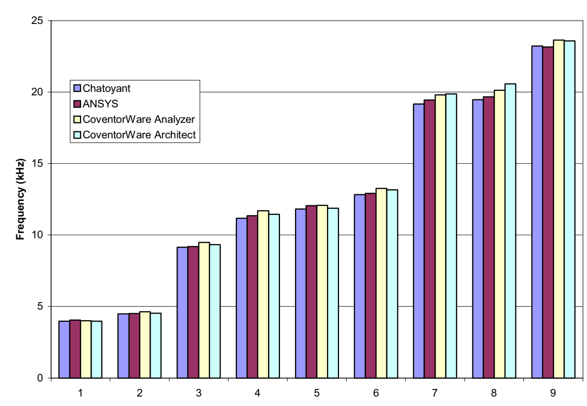

Figure 4: Modal Response of Four Meander Spring

Simulation Time - Spring Modal Analysis		
Solver	Simulation Time	Notes
Chatoyant	1.107 seconds	Two Nodes per Element with Six Degrees of Freedom per Node
CoventorWare Architect	2.330 seconds	Nonlinear - One Segment Beam with Six Degrees of Freedom at Each Beam End
CoventorWare Analyzer FEM*	134.000 seconds	Manhattan Bricks - 27-Node Parabolic Elements (1664 Elements)
ANSYS FEM*	30.000 seconds	3-D 20-Node Structural Solid Element, Solid95 (1664 Elements)
*The FEM Element size is 2.5um x 2.5um x 2um		

Table 2: Simulation Times for Modal Analysis

3.4 Dynamic Behavior of RF Switch

The dynamic response of the switch was investigated in Chatoyant by applying a time-dependent force in the z-direction. A force of 1µN was applied to the plate structure over two different time sequences. The first dynamic response was based on a ramped input of 600ms (Figure 5). The second dynamic response was based on a ramped input of 600µs (Figure 6).

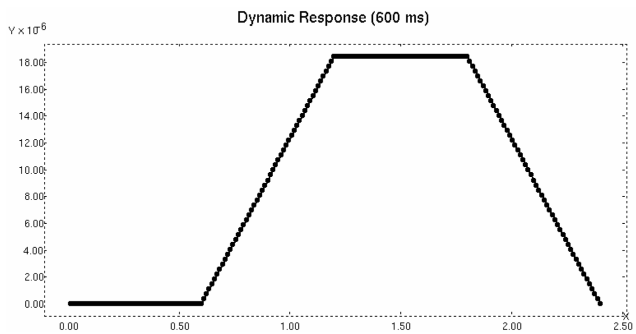

Figure 5: Slow Switch Response (600ms Rise Time)

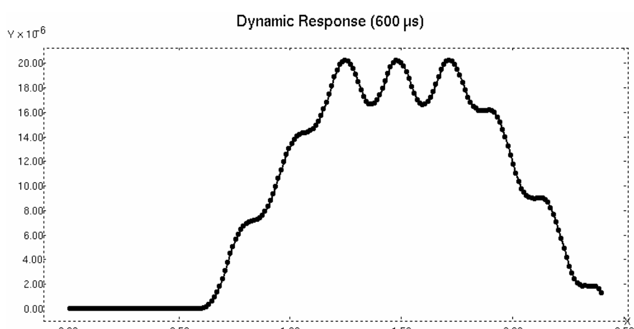

Figure 6: Fast Switch Response (600µs Rise Time)

With a slow input time of the force, the displacement of the switch displays a linear response. Increasing the input speed of the force by a magnitude of 100x, results in oscillations in the device. These oscillations could cause unwanted changes in the capacitance values during actuation. Considering this input force necessitates finding an input frequency which does not result in switch displacement resonance.

4 ELECTROSTATIC MODELING

For the ongoing analysis, the electrostatic models of the device will be investigated. The main factor in the electrical properties of the model stems from the pull-in voltage analysis. Analytically, pull-in voltage is related to the geometry of the parallel-plate capacitor and the stiffness coefficients of the spring meanders.

$$V_{pi} = \sqrt{\frac{8K_z g_o^3}{27\varepsilon_o A}} \tag{2}$$

In the above equation, K_z is the total spring stiffness of the structure (equal to $4*k_z$, where k_z is the individual spring constant), g_o is the initial gap between the switch and the electrodes above the substrate, and ε_o is the free-space permittivity, and A is the area of the actuation plates. The pull-in equation is a result of equating the spring stiffness to the electrical spring softening k_e, where:

$$k_e = -\frac{dF_e}{dz} \tag{3}$$

and,

$$F_e = \frac{1}{2}V^2\frac{dC}{dz} \tag{4}$$

The electrical force is directly related to the parallel plate capacitance of the actuation pads and to the square of the input voltage.

The main concept of the RF switch of this type is to create low-voltage actuation. From the pull-in equation (2), it can be seen that the pull-in voltage can be altered by manipulating any of the geometrical aspects of the switch, namely, the initial gap, the area of the actuation pads, or by increasing the number of meanders in the spring (thereby lowering the overall spring constant).

5 FUTURE WORK: FULL SYSTEM LEVEL SIMULATION

The full system level analysis involves an end to end simulation of the device (Figure 7).

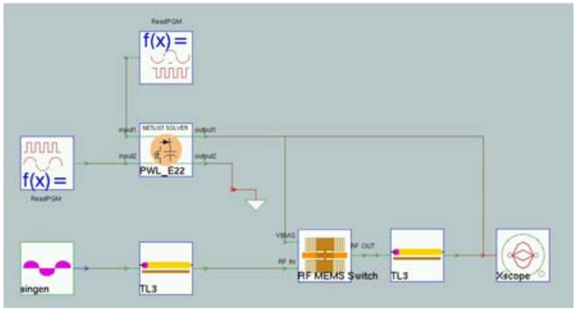

Figure 7: Chatoyant Schematic of Full System Simulation

The system, which uses a high frequency input signal (40GHz – 'singen' block), will be sent along the coplanar waveguide transmission lines (TL blocks). The device will be actuated by a pulsed input (PWL block and signal drivers). The speed of the switching device and the 'shunting' capabilities will be investigated to test the qualities of the device.

6 SUMMARY AND CONCLUSION

The ongoing analysis of the RF MEMS switch requires the capability to cross the mechanical and electrical domains in order to accurately model the device. The meander spring assembly determines the overall stiffness of the structure. The modal response helps to determine the frequency at which the device can be actuated. Dynamic analyses of the device were completed to investigate the switching capabilities of the device.

Other considerations for future analyses are to incorporate residual stresses associated with the fabrication of the device. This includes curvature of the device when released during the etching phase and differences in the geometry of the switch arising from fabrication and design.

REFERENCES

[1] S.P. Levitan, et al, "System Simulation of Mixed-Signal Multi-Domain Microsystems With Piecewise Linear Models." IEEE Trans. On CAD. Vol. 22 n. 2, Feb. 2003, pp. 139-154.

[2] S.P. Pacheco, et al, "Design of low actuation voltage RF MEMS switch," in IEEE MTT-S Int. Microwave Symp. Dig., vol 1, June 2000, pp. 165-168.

[3] Peroulis, D., et al, "Electromechanical Considerations in Developing Low-Voltage RF MEMS Switches," in IEEE Trans. On Micro. Theory and Techniques, vol 51, no. 1, Jan 2003, pp. 259-270.

[4] Yao, J. Jason, "RF MEMS from a device perspective," in J. Micromech. Microeng., vol. 10, 2000, pp. R9-R38.

[5] Przemieniecki, J.S. Theory of Matrix Structural Analysis., Dover Publications, Inc. New York, 1985.

[6] ANSYS Multiphysics/LS-DYNA, ANSYS Inc., Cannonsburg, PA. www.ansys.com.

[7] CoventorWare version2003.1, Coventor, Inc., Cary, NC. www.coventor.com.

Acknowledgements:
This work was supported, in part, by DARPA/AFOSR under grant number F49620-01-1-0536 and NSF under grant number C-CR9988319. The authors would like to thank Coventor, Inc. for their support, advice, and cooperation.